Mineral dust and lead deposition from land use and metallurgy in a 4800-year-old peat record from the Central Alps (Tyrol, Austria)

Clemens von Scheffer, François de Vleeschouwer, Gaël Le Roux, Ingmar Unkel

Mineral dust and lead deposition from land use and metallurgy in a 4800-year-old peat record from the Central Alps (Tyrol, Austria)

Clemens von Scheffer[a,c,d,], François De Vleeschouwer[b], Gaël Le Roux[c], Ingmar Unkel[a,e]*

[a] Institute for Ecosystem Research, Christian-Albrecht University, Olshausenstraße 75, D-24118 Kiel, Germany
[b] Instituto Franco-Argentino para el Estudio del Clima y sus Impactos (UMI IFAECI/CNRS-IRD-CONICET-UBA) Dpto. de Ciencias de la Atmosfera y los Oceanos, FCEN, Universidad de Buenos Aires Intendente Guiraldes 2160 - Ciudad Universitaria (C1428EGA) Ciudad Autonoma de Buenos Aires, Argentina
[c] Laboratoire Écologie Fonctionnelle et Environnement, Université de Toulouse, CNRS, Toulouse INP, Université Toulouse 3 - Paul Sabatier (UPS), Toulouse, France
[d] Geography and Environment, School of Geosciences, University of Aberdeen, St Mary's Building, Aberdeen AB24 3UF, UK
[e] Institute of Geography, Heidelberg University, Im Neuenheimer Feld 348, D-69120 Heidelberg, Germany

* Corresponding author.

E-mail address: clemens.vonscheffer@abdn.ac.uk (C. von Scheffer).

Abstract

Humans have occupied the Alps over most of the Holocene. Yet, continuous records on the impact of using montane resources and landscapes are scarce or confined to segregated areas or periods. We present a high-resolution geochemical record of the last 4800 years from the ombrotrophic peatland Piller Moor in the Central Alps (Tyrolean Oberland, western Austria), using inductively coupled mass plasma spectrometry (ICP-MS) and highly efficient inter-calibrated portable X-ray fluorescence analysis (pXRF). Fluctuations of metal enrichment factors (EF) for lead (Pb), copper (Cu), zinc (Zn) and antimony (Sb), accumulation rates of anthropogenic lead (Pb_{anth} AR) and mineral matter (MAR), based on titanium (Ti), are in line with archaeological and pollen evidence for human presence and environmental change. Periods of intensified, erosive land use are indicated by MAR around 4400 cal BP, 3400 cal BP and, very prominently, at 2400 cal BP. After low MAR in the early Middle Ages, soil disturbances reappear around 1200 cal BP (750 CE), after 200 cal BP (1750 CE) and during the 20th century CE. We found evidence that metallurgy was practised in the area as early as 4450 cal BP, again from 3500 to 2900 cal BP and episodically between 2400 and 1400 cal BP. The Central Alps were presumably a source of increased Pb-emissions in the post-Roman period from 1500 to 1400 cal BP (450–550 CE). Generally, our findings suggest that mining predates archaeological and historical evidence. Following a continuous increase since the Middle Ages, atmospheric Pb EF and Pb_{anth} AR peak around 1980 CE. The record of mineral atmospheric input illustrates the notable impact of human activities on soil erosion and dust entrainment in the Central Alps. Furthermore, links between Little Ice Age cold phases and reduced human impact and mining are established. Our high-resolution peat-geochemistry data quantifies atmospheric deposition of mineral matter and Pb, which act as proxies for landscape evolution and metallurgy on a local and regional scale. It provides new insights and a deeper understanding of the interaction of climate, environment and humans in mountainous landscapes like the Central Alps.

Keywords: Alps; Prehistoric metallurgy; Land use; Peat geochemistry; Atmospheric dust; Portable XRF

1. Introduction

Ombrotrophic peatlands are precious palaeoenvironmental archives. Specific characteristics render them reliable geochemical records of certain contaminants like lead (Pb), copper (Cu) or Antimony (Sb) as industrial or metallurgical emissions (Damman, 1978; De Vleeschouwer et al., 2007; Forel et al., 2010; Jones and Hao, 1993; Nieminen et al., 2002; Shotyk, 1996; Shotyk et al., 2004). They also act as archives of fluctuating mineral atmospheric dust deposition, indicating droughts, storminess or changes in land cover and land use (e.g. Chambers et al., 2012; Hölzer and Hölzer, 1998; Lomas-Clarke and Barber, 2007; Schofield et al., 2010).

Yet, such geochemical studies are rare in the Central Alps, because mires in mountainous landscapes are rather small, heterogeneous, and often disturbed by livestock and drainage (Spitale, 2021; Yang et al., 2017). Furthermore, they are affected by natural geomorphological processes or events and peat accumulation can be low due to short vegetation periods.

When reconstructing human impact and interaction with mountain landscapes, considering proximate archaeological sites is imperative and a key to proper interpretation. The Piller Moor (Tyrol, Austria, Figure 1) is one of the rare, well-preserved ombrotrophic peatlands in direct vicinity to well-known archaeological sites, which are a bronze-hoard and a ritual fire site (Heiss, 2008; Tomedi, 2012, 2002a; Tschurtschenthaler and Wein, 2002). Palynological data is available for the site (Hubmann, 1994), while nearby palaeovegetation studies give a good perspective on regional developments (e.g. Festi et al., 2014; Grabherr, 2006; Wahlmüller, 2002; Walde, 2006). Reconstructions of glacier activity and tree line changes from the nearby Kauner Valley (Figure 1) further provide insight on past regional climate variability during the late Holocene (Nicolussi et al., 2005; Nicolussi and Patzelt, 2000). Although the Eastern Alps became an important mining district during the Bronze Age (O'Brien, 2015; Stöllner and Oeggl, 2015), there is little known on prehistoric mining activity for this area of the Central Alps (Krause, 1987; Stöllner, 2015).

In our study, we use geochemical ICP-MS and portable XRF (pXRF) data to identify periods of metallurgy and to assess the degree and scale of human impact at the junction between the Eastern and Western Alps. Portable XRF can be a time and cost-efficient tool to analyse the chemistry of a wide variety of materials (e.g. Kalnicky and Singhvi, 2001; Liritzis and Zacharias, 2011; Palmer et al., 2009). However, palaeoenvironmental studies using pXRF remain scarce (Gałka et al., 2017; Kapustová et al., 2018; von Scheffer et al., 2019). One of the challenges is that preinstalled calibrations rarely cover the highly organic sample matrix of peat. Hence, we developed an (inter)calibration between semi-quantitative

pXRF and ICP-MS measurements, following full acid digestion in a clean room. Certified reference materials (CRM) for both methods act as an independent verification of the quality and reliability of our approach. Our geochemical proxy data is supported by pollen data from the same site (Hubmann, 1994) and other local palynological and archaeological studies, providing a comprehensive picture of regional human land use, metallurgy and environmental conditions in the past.

2. Methods

2.1 Study area and site

As part of the Tyrolean Oberland, the climate at the Piller Moor is alpine-continental with a mean annual precipitation of ca. 800 mm and main wind directions are between west and south (46%) and north to north-east (18.5%) for the period between 1971 and 2000 CE in Landeck (Central Institution for Meteorology and Geodynamics of Austria, (ZAMG, 2018)). The Piller Saddle is in the altitudinal lower subalpine zone (c. 1550 m a.s.l.). The Inn River (c. 800 m a.s.l.) approaches the Piller Saddle from the South before joining with the Sanna River at Landeck and turning east (Figure 1). The Kauner, Pitz and Oetz Valleys are south-east of the Saddle. A brook (Pillerbach) drains the mire in north-easterly direction over the Pitze River into the Inn Valley, which divides the Penninic metamorphic zone to the south and the northern Limestone Alps.

The Piller Moor lies within a depression at 1540 m a.s.l., stretching approx. 380 m W to E and 30 to 100 m N to S, with the water-level at approx. 10 cm below surface. *Sphagnum* spp. dominates the vegetation, together with *Andromeda polifolia, Drosera spp., Cyperaceae* and *Pinus mugo rotundata* stands towards the periphery, which is typical for ombrotrophic mires. The surrounding forest consists of *Picea* spp.*, Pinus* spp. and *Larix* spp.

2.2 Coring and sub-sampling

Coring in the Piller Moor took place in 2017. For the profile Pi17 (47°07’24.85” N, 10°39’45.45” E), a Wardenaar system (10x10 cm; Wardenaar, 1987) was used to core the top meter of the mire and a piston corer (Usinger 8 cm barrel; Mingram et al., 2007) was used for the deeper layers. Parallel profiles (A and B) were taken to get a composite core. A maximum depth of 380 cm was reached before hitting an impenetrable layer, supposedly consisting of woody material. The segments were wrapped in cling film, transferred into a PVC-casing and sealed in a plastic hose. Cores A and B were sliced continuously to subsamples of c. 1.1 cm thickness for geochemistry and dating. Dry bulk density was calculated using the dimensions and dry weight of the geochemistry samples. Clean coring and subsampling followed the protocol of De Vleeschouwer et al. (2010) and Givelet et al. (2004). Three macrofossil samples were

picked in ultrapure water for radiocarbon dating at Poznan AMS Radiocarbon Laboratory (Poz), Poland. Other samples were selected with the same method, pre-treated at the Gliwice Radiocarbon Laboratory (GdA), Poland and measured at the Rafter Radiocarbon Laboratory, New Zealand.

2.3 Geochemistry

143 dry samples for pXRF and 63 samples for ICP-MS analyses, were selected and processed following Le Roux and De Vleeschouwer (2010). The samples were crushed to a homogenous powder in 15–50 ml tubes with eight glass beads of 4 mm using a FastPrep®-24 ball-mill (3x20 s at 6 $m*s^{-1}$). For pXRF-analysis, sample and CRM preparations and measurements were done on dried and homogenised peat, following the protocol in von Scheffer et al. (2019). The samples were transferred into polystyrene containers, covered with 4-µm thick polypropylene film and measured using a handheld Thermo Fisher Scientific Niton Xl3t, inside a test stand. The pXRF-device was rebooted regularly to account for fluctuations of temperature and atmospheric pressure during the day. The Xl3t was used in soil-mode, running the main and low-filter for 180 s each.

Samples for ICP-MS analyses were digested in a class 100 clean room at „Laboratoire Ecologie Fonctionnelle et Environnement“ Toulouse, France. Following the protocol for acid-digestion of peat samples detailed in Vanneste et al. (2015), 100 mg peat powder was treated consecutively with ultrapure chemicals, first with 2 ml of 65 % nitric for 24 h at room temperature and, after adding 0.5 ml hydrofluoric acid, at 110 °C for 48 h, then with 31 % ultrapure peroxide at room temperature for 24 h and lastly in 2 ml 65 % nitric acid at 110 °C for 48 h. Before every step, the mix of dried sample and liquid was treated with ultrasound and the samples were evaporated at 50 °C in between steps. An In/Re spike was added to each sample. Five multi-element standards were run every 10 samples to correct for instrument drift. A blank and two different organic CRMs (NIST-1547a, NIST-1515, GBW-07603, NJV-942, NJV-941) were treated per batch of 21 samples and measured in regular intervals. In addition to the CRMs used in ICP-MS, BCR-060, IAEA-336, IPE-176 and NIST-1575a were used for pXRF.

2.4 Computing and calculations

The calculations and regression analyses are performed in R version 4.0.3. (R Core Team, 2021). The Bayesian age-depth model (ADM) is created using the package *rbacon* version 2.5.3 (Blaauw and Christen, 2011) with a 95 % confidence interval and the IntCal20 radiocarbon calibration curve (Reimer et al., 2020). Boundaries are added based on obvious changes in density and humification. Median ages are given as ‘cal BP’ (calibrated years before 1950). Historical or certain cited ages are given as

CE. The peat accumulation rate represents the bulk thickness of one peat sample and the period of time covered (Δthickness/Δtime) in mm*year^{-1}.

Metal enrichment factors (Me EF) for Pb, Sb, Cu and Zn and atmospheric mineral accumulation rates (MAR) are calculated using the conservative behaviour of Ti in peat (Nesbitt and Markovics, 1997), as done in Shotyk et al. (2002), to detect past metal enrichment and land use change (e.g. Kempter et al., 1997). The choice of Ti was also pre-determined by the range of elements of the pXRF. Pb, Sb, Cu, and, sometimes, Zn are commonly used to trace metallurgical or industrial emissions (e.g. Damman, 1978; Jones and Hao, 1993; Nieminen et al., 2002; Shotyk, 1996; Shotyk et al., 2004).

$$Me\ EF = \frac{\left({}^{Me}/_{Ti}\right)_{Sample}}{\left({}^{Me}/_{Ti}\right)_{UCC}}$$

$$MAR = {}^{100}/_{0.41} * Ti_{Sample} * \delta * \mathrm{PA}$$

δ is the dry bulk density and PA is the peat accumulation rate.

An anthropogenic Pb accumulation rate (Pb_{anth} AR) is calculated following Weiss et al. (1999). First, the concentration of Pb in local and natural soil dust (Pb_{nat})are determined for every sample.

$$Pb_{nat} = Pb_{Sample} * \left({}^{Pb}/_{Ti}\right)_{UCC}$$

Pb_{nat} is then subtracted from every sample to obtain the anthropogenic contribution $Pb_{anth.}$, which is then used to calculate Pb_{anth} AR as follows:

$$Pb_{anth.}AR = Pb_{anth.} * \delta * \mathrm{PA}$$

The upper continental crust (UCC) concentrations (McLennan, 2001) are used as reference or background values to calculate MAR, metal EFs and Pb_{anth} AR with Ti (4100 mg*kg^{-1}), Pb (17 mg*kg^{-1}), Cu (25 mg*kg^{-1}), Zn (71 mg*kg^{-1}) and Sb (0.2 mg*kg^{-1}). Using the UCC-values is partly because of the heterogenous geology of the Alps and their surroundings as potential dust sources, but it also makes the results more comparable to similar studies. Furthermore, the mineral base was not reached to get a local sediment reference and defining a natural reference level within our samples would be difficult within the age range of the peat record.

Model estimates are made in all unmeasured peat samples from the continuous profile by linear interpolation between measurements. These modelled data-points are of course not included in the main data and figures, but they allow a simple approximation of the cumulative anthropogenic Pb-deposition and of both the average MAR and Pb_{anth} AR over time.

The chronological interpretations are separated into five different periods from Neolithic until present, which largely correspond to cultural periods in the central Alps, also used by Röpke et al. (2011).

3. Results

3.1 Chronology

Sphagnum spp. mosses dominate throughout the core sections. The deepest section of profile B was fitted and merged to the deepest section of profile A, using density, geochemistry and radiocarbon dates (Table 1).

The age-depth-model (Figure 2) provides a median age of 4750 cal BP for the core bottom. Up to 182 cm depth (2000 cal BP), the peat accumulation rate (AR) remained mostly below 0.7 $mm*a^{-1}$ before increasing to 0.8-1.2 $mm*a^{-1}$ until 91 cm (1200 cal BP). A significant decrease to less than 0.4 $mm*a^{-1}$ prevails from 91–61 cm (1200–100 cal BP). In the uppermost part, the AR increases to over 10 $mm*a^{-1}$. The most recent part of the model relies upon a single bomb-pulse date (GdA-5492), which reduces the uncertainty in the upper 50cm.

3.2 Geochemistry

Dry bulk density, raw pXRF and ICP-MS results (data vs depth and calibrated ages) are given in Table SI_1. The raw data output of the analyses is presented as ICP-MS vs pXRF (Figure 3) for the purpose of visual comparison and performing regression analyses.

3.2.1 Quality control

The data relevant for quality control is provided in the supplementary information (Table SI_1). Concentrations in the blanks attest clean sample processing. Measurements of Ti, Pb, Zn, Rb, K, Sb, Fe, Sr and Cu deviate less than 20 % from certified values in ICP-MS. In contrast, raw pXRF results of the CRMs are generally much higher than their certified concentrations. Yet, only the pXRF-measurements of Cu, Zn, and K show standard deviations (sd) over 20 % in certain organic CRMs (e.g NJV-941).

Elements that are not detectable with pXRF in most samples, for example due to detection limits, or which produced arbitrary results, were not considered further in the regression analysis. This is the case for Cu and Sb leaving only Fe, K, Pb, Rb, Ti, Zn and Sr for further use.

3.2.2 Regression Analysis

von Scheffer et al. (2019) demonstrate the general reliability and cost and time efficiency of pXRF analyses for Ti and Pb in peat. In the same way, we here performed an individual regression analysis of pXRF versus ICP-MS and CRMs on a broader set of elements. The regression functions of CRMs, ICP-MS and pXRF-results (Figure 3) show a good linear fit for Ti (R^2=0.98), Pb (R^2=0.99), Sr (R^2=0.99), K (R^2=0.98), Rb (R^2=0.97), Zn (R^2=0.92) and Fe (R^2=0.86). Although pXRF-results are above certified values, these elements can be cross-calibrated with quantitative methods or by using appropriate organic CRMs. Depending on the elements in question, a regression analysis could be based on a larger set of CRMs alone (red symbols in Figure 3).

3.2.3 Elemental profiles

The relevant concentration vs depth profiles (Figure 4) and further interpretation are based on the pXRF data calibrated for quantification via ICP-MS using the regressions (Figure 3). The pXRF profiles have a higher depth resolution, except for Cu and Sb which were only measured by ICP-MS (Figure 4).

Peaks in Ti exceeding 400 mg*kg^{-1} and 600 mg*kg^{-1} appear at 312.5 and 200 cm (4140 and 2330 cal BP), respectively, with some minor peaks of 400 mg*kg^{-1} and 260 mg*kg^{-1} at 88 cm and 62 cm (1050 and 110 cal BP). Rb resembles the course of Ti, staying mostly below 5 mg*kg^{-1} except for the five peaks parallel to Ti, indicating stronger terrigenous influx into the mire during these periods. A slight increase in Rb is also recorded in the surface layers. K ranges between 300 and 700 mg*kg^{-1}, with peaks at 312.5 cm (3000 mg*kg^{-1}) and again at 200 cm, followed by 2300 and 1500 mg*kg^{-1} at 88 cm and 62 cm. A rising trend shows in the uppermost 25 cm. Sr gradually rises from 10 mg*kg^{-1} to a maximum of 30 mg*kg^{-1} at 200 cm (2330 cal BP). After a local minimum of 2 mg*kg^{-1}, a declining trend sets in at 155 cm (1770 cal BP). Fe doubles from 1500 mg*kg^{-1} at the bottom to approx. 3000 mg*kg^{-1} at 125 cm depth before decreasing again.

Pb concentrations remain low around 3 to 10 mg*kg^{-1} between 350 and 100 cm (4710–1260 cal BP). An increase to 20 mg*kg^{-1} appears around 328 cm. In three subsequent peaks in the uppermost metre, the maximum concentration increases from 35 mg*kg^{-1} at 90 cm (1120 cal BP) to 70 mg*kg^{-1} at 39 cm (-29 cal BP). Cu peaks at 326 cm (39 mg*kg^{-1}) and 282 cm (23 mg*kg^{-1}). Smaller increases appear at 310, 262 and 200 cm. However, a decreasing trend is obvious towards the surface. Sb increases to 3 mg*kg^{-1} at 326 cm but is mostly below 1 mg*kg^{-1} until 90 cm. A maximum of 7 mg*kg^{-1} at 67 cm is followed by concentrations over 1 mg*kg^{-1}. Zn is on a level between 10 and 20 mg*kg^{-1}, rises to c. 30 mg*kg^{-1} at 312.5, 270, 200 and 62 cm (4140, 3500, 2330 and 110 cal BP) and exceeds 40 mg*kg^{-1} near-surface.

The dry bulk density gradually increases from 0.05 to 0.1 g*cm^{-3} in the lowest 100 cm and sharply returns to 0.05 g*cm^{-3} at 250 cm. A density peak to over 0.1 g*cm^{-3} covers 90 to 62 cm.

3.2.3 Accumulation rates and enrichment factors

MAR stays mostly below or around 1.5 g*a^{-1}*m^{-2}, but remarkable peaks of c. 9 g*a^{-1}*m^{-2} appear at 2350 cal BP and again in in the last century (Figure 5). Moderate increases in MAR appear prior to 4000, and around 3400, 1600, 1100 and 200 cal BP.

A peak of Pb_{anth} AR around 4400 cal BP (approx. 0.8 mg*a^{-1}*m^{-2}) is followed by a slowly rising trend from 4000 until 3250 cal BP to 0.5 mg*a^{-1}*m^{-2}. After another single peak around 1450 cal BP (approx. 0.7 mg*a^{-1}*m^{-2}), Pb_{anth} AR values are constantly elevated after 1200 cal BP. An extreme peak occurs for both Pb_{anth} and Pb EF between 50 and -50 cal BP (1900–2000 CE), corresponding to 30 mg*a^{-1}*m^{-2} and an enrichment over 300. EFs of Zn, Cu and Sb show smaller increases along the profile, but rise strongly in the top layers corresponding to the 20th century CE. Cu EF shows a continuously declining trend until approx. 1000 cal BP.

In Table 2, the estimated averages of accumulation rates as well as the estimated cumulative loads of Pb_{anth} during the five periods (discussed in section 3.3) are summarised.

4. Peatland and landscape evolution and human impact

4.1 Trophic status and atmospheric input

The low dry bulk density and low concentrations of Sr paired with the observed *Sphagnum* spp. Dominance suggest ombrotrophic conditions over the full profile Although the Sr-concentration profile fluctuates from top to bottom, it does return to low concentrations in the deepest section of our record, which is unlike a typical profile of a fen. Furthermore, the deepest section of the peat record is not the mineral bottom, as we hit an impenetrable layer of wood. Rather gentle slopes around the peatland and the fact that the core was taken in the peatland's centre, makes surface input unlikely. Even with a spatially restricted higher availability of nutrients from the more mineral rich layers (e.g. 60-90 cm and 200 cm), which would favour other Sphagnum species or more vascular plants, the main elements used for interpretation (Ti, Pb) show a generally conservative behaviour in peat. While the immobility of Ti is well accepted and often used as a conservative reference element (Bao et al., 2012; Sapkota et al., 2007; Shotyk et al., 2002), Pb also remains largely immobile even when affected by strongly fluctuating water tables (Rothwell et al., 2010) and it shows the strongest adsorption to organic matter in peat (Koivula et al., 2009; Krumins and Robalds, 2015). In contrast, the increasing trend of Cu with depth could indicate some mobility, which is why it is interpreted with caution.

On first sight, Pb_{anth} AR and Pb EF (figure 5) can appear inconsistent when, for example, anthropogenic Pb input is masked (diluted) by local soil dust input with a low natural background signature. Or, during times of low energy dust entrainment and deposition (MAR), the consequently finer particles could bear higher concentrations of Pb or trace metals (Shotyk et al., 2002; Ujević et al., 2000). The former can be assumed when Pb_{anth} AR is high and Pb EF low. The latter is to consider with Pb_{anth} AR being low and Pb EF high. Pb-enriched atmospheric dust could also be more distal or very small, and therefore not increasing significantly the total accumulation significantly. With simultaneously rising Pb_{anth} AR and Pb EF, and especially in prehistoric times, local or regional metallurgy is very likely. In any event, most of the interpretation is based on the more robust Pb_{anth} AR.

4.2 Neolithic-Bronze Age transition (Period 1 from 4800 to 4000 cal BP)

Land use: Increases of mineral matter input at 4450 and 4150 cal BP from less than 0.5 to c. 2 and 5 $g*a^{-1}*m^{-2}$, respectively, are in line with indicators for forest clearances, increased pastoralism indicators and burning in the area (Hubmann, 1994; Walde, 2006). Wahlmüller (2002) suggests first human impact in the region near Serfaus southwest of the Piller Moor around 4250 cal BP.

Around the same time, agricultural terraces (Zoller et al., 1996) and alpine pasture systems (Reitmaier, 2012) emerged in other areas of the Central Alps. Dietre et al. (2014) report increasing charcoal values and agricultural evidence from 4400 to 4200 cal BP in the Fimba Valley. Bortenschlager (2010) documents tree cover loss and cultural pollen at 4400 cal BP, and Dietre et al. (2017) suggest fire management in the lower Engadine, Switzerland.

From a climatic perspective, the peaks in MAR around 4450 and 4150 cal BP coincide with minimum glacier stands in the region (Nicolussi and Patzelt 2000). Afterwards, a continuously declining tree line in the Kauner Valley (Nicolussi et al., 2005) could have resulted from both climate and human forcing and contributed to an increasing trend of MAR, starting around 4000 cal BP. Yet, it is still the period with the lowest estimated average MAR (1.01 $g*a^{-1}*m^{-2}$, Table 2).

Metallurgy: Only few hints for prehistoric mining exist in western Tyrol (e.g. Grutsch and Martinek 2012). Even the ancient mining districts of the Eastern Alps bear only limited evidence before 3750 cal BP (O'Brien, 2015), although copper mining could have started around 4450 cal BP (Knierzinger et al., 2021, 2020). Metallurgy in general was already present in the Alps at that time (Höppner et al., 2005). Ore extraction is suggested for the Southern Alps (Artioli et al., 2016) and Cu-mining is suggested for the Eastern Alps (Knierzinger et al., 2020). In the Piller Moor record, an increase of Pb_{anth} AR to 0.8 $mg*a^{-1}*m^{-2}$ between 4500 and 4200 cal BP is the highest until the end of the Middle Ages. This pronounced signal also coincides with synchronously enriched Pb and Sb and with the MAR and pollen indicators mentioned above, which suggests a link between these proxies of human impact. A lake record to the south-west (Meidsee) (Thevenon et al., 2011) shows Pb-isotope supported evidence for

metallurgy, which shows that the technology was around. However, the coincidence of proxies with the marked rise of Pb_{anth} AR indicates that the inputs of the Piller Moor peat record had a proximate source at that time. Various polymetallic ore deposits in the area contain Cu, Ag, Pb, As and Sb, and some had been exploited over the last millennium (Grutsch and Martinek, 2012; Hammer, 1915; Hanneberg et al., 2009; Neuhauser, 2015; Vavtar, 1988; Weber et al., 1997). Local small-scale metallurgy is therefore likely, but it would predate any direct archaeological evidence and the possibility of remote transport cannot be ruled out completely. Despite the depth, influence of minerotrophic conditions on the estimated Pb_{anth} AR average of 0.26 $mg*a^{-1}*m^{-2}$ (Table 2) is unlikely, as the described Pb-peak is very distinct from the background level and the Sr-concentration profile is very low.

4.3 Bronze Age (Period 2 from 4000 to 2800 cal BP)

Land use: Towards 3400 cal BP, increasing land use activity is suggested by rising MAR, which is in good agreement with *Cerealia* pollen in the Piller mire (Hubmann 1994) as well as open landscape and pastoral indicators in nearby study sites (Wahlmüller, 2002; Walde, 2006). Coinciding elevated charcoal values in these studies are in line with an increased fire clearance in the Alps (Valese et al., 2014).

Local archaeological evidence of Bronze Age buildings in Fließ (Tomedi et al., 2009) and Kaunerberg (Staudt and Tomedi, 2015), and the ritual site on the Piller Saddle dating between 3450 and 3230 cal BP (Tschurtschenthaler and Wein, 2002, 1998, 1996), indicate extensive human activity in the study area, which was probably responsible for the doubling of the estimated average MAR (1.94 $mg*a^{-1}*m^{-2}$).

A pulse of stronger human activity is also evident in other regional records from the Central Alps (Dietre et al., 2014; Festi et al., 2014; Röpke et al., 2011; von Scheffer et al., 2019). In the Eastern Alps, intensified human impact is documented (Knierzinger et al., 2020; Viehweider et al., 2013), possibly to sustain copper mining operations (Stöllner, 2015).

Following on glacier progression around 3600 cal BP, a recession until 3350 cal BP (Nicolussi et al., 2005) could have promoted land use at higher elevations mentioned earlier. Inferred from low MAR and pollen (Hubmann, 1994; Walde, 2006), local and regional land use declined after 3200 cal BP, possibly induced by a cooling trend (e.g. Ivy-Ochs et al., 2009).

Metallurgy: Slightly elevated but fluctuating EFs for Pb, Cu and Zn are recorded between 3750 and 3450 cal BP, while Pb_{anth} AR slowly rises to 0.5 $mg*a^{-1}*m^{-2}$ until 3400 cal BP, before dropping again (Figure 5). Compared to sites in the Vosges, Alpine Foreland and Swiss Jura, with max. Pb_{anth} ARs of c.

0.2, 0.016 and 0.075 mg*a^{-1}*m^{-2} respectively (Forel et al., 2010; Kern et al., 2021; Shotyk et al., 1998), the estimated average of 0.33 mg*a^{-1}*m^{-2} in our record is considerably higher during this period. Not far from the Piller Saddle, Bronze Age ceramic mixed with copper slag found near a malachite ore deposit suggests local metallurgy and mining (Tomedi, 2002b). A large Middle or Late Bronze Age bronze hoard and unworked copper were found nearby (Tomedi, 2012, 2002a, Nicolussi Castellan et al., 2008). The chemical signature of this hoard's artifacts largely corresponds to the well-studied Mitterberg mining district in the Eastern Alps (Pernicka et al., 2016), although the main wind directions make trajectories from there to the Piller Moor less likely. In any case, the lack of characterisations (e.g. isotopy, composition) of local polymetallic ores around the Piller Moor makes tying any artifacts to nearby sources impossible. A Pb-isotope record from a peatland in southern Germany suggests Iberian ores as the main source of atmospheric Pb fluxes during this time (Kern et al., 2021). However, more proximate and thus more likely source regions like the Alps or Black Forest, have not been considered so far. The behaviour of Pb EF and AR is challenging to interpret in this period and pointing out a source even more, but the combined evidence suggests that metallurgy was practised regionally.

4.4 Iron Age (Period 3 from 2800 to 2000 cal BP)

Land use: Around 2400 cal BP, Hubmann (1994) reports increased abundances of charcoal, *Plantago spp., Poaceae, Cyperaceae* and *Cerealia* at the Piller Moor as evidence of land use change, fitting to similar palaeoecological signals of increased human impact at Fließ (Walde, 2006) and Serfaus (Wahlmüller, 2002). The drastic rise of MAR to more than 9 g*m^{-2}*a^{-1} illustrates the intense human impact, with strong deforestation and agro-pastoralism, followed by heavy soil destabilisation. Archaeological sites on and around the Piller Saddle show widespread human occupation in this area (Lutz and Schwab, 2015; Staudt, 2011; Sydow, 1995; Tschurtschenthaler and Wein, 2002; Zemmer-Plank, 1992), explaining the strong impact on the Piller Moor .

Metallurgy: Pb EF does not suggest local metallurgical activity during the early Iron Age. However, strong mineral input masked increased Pb input around 2400 cal BP. This is shown by simultaneously elevated Pb_{anth} AR, which remains on a higher level afterwards. This period has the lowest estimated average Pb_{anth} AR with 0.16 mg*a^{-1}*m^{-2}, but the trend largely agrees with records from Black Forest, and the Vosges (Forel et al., 2010; Le Roux et al., 2005). Although direct evidence is lacking for the Central Alps, silver production as early as 2250 cal BP is suggested for the Swiss Wallis (Guénette-Beck et al., 2009), making also local mid or late Iron Age metallurgy in the study area a possibility.

4.5 Roman Period to Early Middle Ages (Period 4 from 2000 to 1400 cal BP)

Land use: In agreement with an initial MAR minimum at Piller Moor, larger forests and reduced pastoralism are reported once the region fell under Roman influence around 1950 cal BP (Bortenschlager, 2010; Hubmann, 1994; Wahlmüller, 2002; Walde, 2006). This is reflected in the estimated average MAR of 1.41 $g*a^{-1}*m^{-2}$ being lower than the pre-Bronze Age and the Iron Age estimated averages (periods 3 and 5). Yet, MAR fluctuations around 1750 cal BP match indicators for burning and landscape openings in Fließ (Walde, 2006). Just prior to a MAR peak around 1660 cal BP, increased charcoal values in the Piller Moor (Hubmann 1994) indicate reoccupation of the higher slopes, coinciding with crisis in the Roman Empire (Wierschowski, 1994).

Walde (2006) and Hubmann (1994) document a significant forest recovery and absence of cultural indicators around 1400 cal BP, when the MAR declines below 1 $g*m^{-2}*a^{-1}$. This gap of human impact agrees with other observations in the Central Alps (e.g. von Scheffer et al., 2019) and is connected to a cold climate extreme referred to as Late Antique Little Ice Age (Büntgen et al., 2016; Helama et al., 2017; Ivy-Ochs et al., 2009).

Metallurgy: Compared to the Iron Age, the mean estimated Pb_{anth} AR of 0.25 $mg*a^{-1}*m^{-2}$ during this period is significantly higher. Elevated Pb_{anth} AR and Pb EF during the earlier part of this period are likely associated with distal origin and diffuse Roman influence (e.g. Longman et al 2020), in contrast to peaks of Pb EF and Pb_{anth} AR (c. 0.7 $mg*a^{-1}*m^{-2}$) around 1450 cal BP. Similar signals are registered across Western and Central Europe, for example in the Bernese Alps (Carvalho and Schulte, 2021), and in the northern Central Alps (von Scheffer et al., 2019), but also in Eastern Europe (Bohdálková et al., 2018). A rise is also visible in the Colle Gnifetti ice (More et al., 2017), but a 90-year gap starts just at this particular age. Kern et al. (2021) attribute this Pb signal to a transition to small scale and local mining operations across Europe, although atmospheric Pb-emissions and deposition were generally reduced during this period (e.g. Forel et al., 2010). Yet, it is striking that neither records from the Southern Alps (Segnana et al., 2020), nor south-west from our site (Thevenon et al., 2011), nor from locations west and north-west of them (Vosges, Black Forest, Massif de Morvan, Swiss Jura), nor from the Eastern Alps (Knierzinger et al 2020), show increased Pb EF or Pb_{anth} AR at that time (Forel et al., 2010; Le Roux et al., 2005; Monna et al., 2004; Shotyk et al., 1998). Considering that the supra-regional Roman Pb-signal is not very defined in our record, the distinct and synchronous Pb EF and AR signals from 1500 to 1400 cal BP suggest an origin rather close to the Piller Moor. This period was a time of warfare and territorial reorganisation, but the Central Alps were not in the centre of these conflicts (Kulikowski, 2012). Late Antiquity silver mining in the Swiss Alps is, however, suggested by Guénette-Beck et al. (2009) and regional Pb and Ag deposits around Imst (Gstrein, 2013), in the Austrian Vorarlberg region (Hofmann and Wolkersdorfer, 2013), and in Tirol (Vavtar, 1988) could have made parts of the Central Alps potential hotspot of Pb-emissions during this particular period.

398

399 ## 4.6 Middle Ages to Postmodernity (Period 5 from 1400 cal BP to present)

400 **Land use and climate:** In line with a rising MAR in our record, Walde (2006) and Hubmann (1994) report
401 a general rise of pastoral, cultural and grassland pollen after 1250 cal BP nearby (see Figure 1). A
402 landscape opening is also observed at Serfaus by Wahlmüller (2002). Still elevated mineral input at 900
403 cal BP coincides with increased charcoal, crops, *Plantago* spp. and decreased tree pollen in the Piller
404 Moor, while lower land use is indicated at c. 650 and 350 cal BP by both MAR in our record and pollen
405 (Hubmann 1994).

406 The gradually declining MAR after 1000 cal BP coincides with glacier advances in the nearby Kauner
407 Valley (Nicolussi and Patzelt, 2000). Consequently, a lower MAR towards the early Modern Period
408 could have resulted from declining mountain farming in the Alps (Lichtenberger, 1965), which Bender
409 (2010) attributes to a cooler climate. In contrast, the MAR peak after 200 cal BP is associated with a
410 temporary surge of expanding local and regional agriculture and forestry. The forest at Kaunerberg (c.
411 5.5 km south of the mire) lost about 140 ha between 1774 and 1880 CE and losses up to 85 % are
412 documented in the nearby Radurschl, Pitz, Oetz and Paznaun valleys (Fromme, 1957). Thereafter,
413 documentation from 1850 to 1951 CE can explain the shrinking MAR: Agricultural yields and livestock
414 declined by 50 % and 40 % respectively (Fromme, 1957). The construction of a tourist infrastructure,
415 high voltage line poles and roads and the subsequent nature conservation measures possibly caused
416 the recent MAR-peak and its decline over the last few decades. Apart from this, the estimated average
417 MAR in this period (3.94 $g*a^{-1}*m^{-2}$) is higher than in any of the previous periods.

418 Lower peat accumulation and higher density observed within the top metre (90 to 62cm) of our record
419 could relate to indirect anthropogenic disturbances, similar to observations of Sjögren et al. (2007).
420 The area was listed as a natural resource (von Klebelsberg, 1939), leading to industrial peat mining in
421 an adjacent bog between 1949 and 1971 CE. A hydrological link to the exploited site could have
422 promoted disturbance in the Piller Moor's surface layers. Recently introduced conservation measures
423 in the area were likely beneficial for a return to previous peat accumulation rates and current growth
424 rates of over 1 $cm*a^{-1}$.

425 **Metallurgy and pollution:** All EFs as well as a sharp rise of the Pb_{anth} AR indicate constant metallurgy
426 in the area after 1200 cal BP (750 cal CE), preceding first historical sources on Ag, Pb and Zn extraction
427 in the 12th century CE (Hanneberg et al., 2009; Wolkersdorfer, 1991) and the awarding of mining rights
428 in 1352 CE (von Srbik, 1929). An increasing Pb EF is also reported from other sites (e.g. More et al.,

2017; Segnana et al., 2020; Thevenon et al., 2011), which illustrates that the development was supraregional and more distal sources likely contributed as well.

By 500 cal BP (1450 cal CE), strongly rising EFs (Pb and Sb) are in line with the introduction of a new and more pollutive ore processing technology (Breitenlechner et al., 2013; Longman et al., 2020). A link to intensifying silver mining around Imst (Hanneberg et al., 2009) and the Arlberg region (Haditsch and Krainer, 1992), north and west of our record, is also likely. South of Piller in Platzertal (Platzer Valley), Pb was mined and smelted from 1538 CE to 1900 CE (Vavtar, 1988). A climate induced temporary abandonment of this mining site (1610–1888 CE) is synchronous with a decreasing Pb EF in our record. In addition, regional mining was outcompeted by overseas' ores (Wolkersdorfer, 1991). The recent maximum of Pb_{anth} AR (c. 30 $mg*m^{-2}*a^{-1}$) and Pb EF (>300) are the result of leaded gasoline emissions (Pacyna and Pacyna, 2001). The sharp drop in the late 1980s is the response to its stepwise reduction and final ban across Europe. Compared to the maximum values in the Alpine Foreland (c. <6 $mg*m^{-2}*a^{-1}$; Kern et al., 2021) and to the records summarised in Forel et al. (2010), which are the Black Forest (c. 14 $mg*m^{-2}*a^{-1}$), Jura (c. 14 $mg*m^{-2}*a^{-1}$) and Vosges (c. 12 and 39 $mg*m^{-2}*a^{-1}$), the maximum Pb_{anth} AR in our record is mostly higher. Whilst the Pb_{anth} AR does not return to natural background levels, it is within the upper range of Pb AR around 1 $mg*m^{-2}*a^{-1}$ recently observed in Central Europe (e.g. Kempter et al., 2010), yet, lower than values in the black triangle of Eastern Germany, Poland and the Czech Republic (e.g. Zuna et al., 2011). Our Pb record is in good agreement with the history of pollution in Central Europe. Its steep decline acts just as another time marker, which is confirming our age depth model. Since our peat profile covers a longer time period, the estimated cumulative anthropogenic Pb-deposition of c. 2.7 $g*m^{-2}$ (Table 2) is slightly higher than in most of the Swiss peat records summarised in Shotyk et al. (2000).

5. Conclusions

Mineral and metal accumulation rates (MAR) and enrichment factors (EF), calculated based on geochemical analyses and combined with other palaeoecological proxies, provide continuous evidence of human occupation when archaeological evidence is lacking or isolated. Past episodes of metallurgy and anthropogenic soil disturbances in the Central Alps are revealed in our Piller Moor record. Methodological evidence shows that pXRF facilitates high-resolution, quantitative data acquisition of certain elements in ombrotrophic peat (Ti, Pb, Zn, Sr, K, Rb, Fe), whereas others (e.g. Cu) cannot be quantified.

Our results suggest mining or metallurgy in the Central Alps between 4500 and 4200 cal BP, predating any archaeological evidence in the area. Around 3400 cal BP, both mineral input and Pb_{anth} AR are elevated synchronously with palynological and archaeological evidence for human activity. A strong

mineral input pulse at 2400 cal BP is simultaneous with proximate palynological and archaeological indicators for heavy human landscape disturbance. Despite Roman presence in the Inn valley, their direct impact at higher elevation seems to have remained small. Temporary but distinct increases of Pb_{anth} AR and Pb EF from 1500 to 1400 cal BP strongly indicate post-Roman mining and metallurgy in this part of the Central Alps, encouraging further research to locate potential sources in the area. However, the anthropogenic impact was very weak in the Early Middle Ages before soil disturbance and metallurgy resumed around 1200 cal BP and did not return to previous levels again. Our data indicate early medieval mining operations, which predate historical documentation by several centuries. While the LIA likely impaired regional agriculture, forestry and mining operations episodically, the comparison of our record to historical documentation highlights the severe influence of expanding forestry and agriculture on regional soil erosion and dust entrainment over the last centuries. Over the last century, nearby peat extraction and construction, but also nature conservation, seem to have influenced mineral and peat accumulation. The abrupt decline of Pb EF and Pb_{anth} AR after the year 1980 CE acts as a time marker. In the form of quantitatively reconstructed atmospheric input, geochemical signals found in our peat record from the Piller Moor mainly reflect the development of local and regional human activities and their impact on the Alpine landscape over the past 4800 years.

Author contributions

Clemens von Scheffer: Fieldwork, Investigation, Data curation, Writing- Original draft preparation, Project administration, Visualisation, Conceptualisation, Methodology, Funding acquisition.: **Ingmar Unkel:** Fieldwork, Conceptualisation, Supervision, Writing- Reviewing and Editing, Funding acquisition.: **François De Vleeschouwer:** Conceptualisation, Methodology, Supervision, Writing- Reviewing and Editing, Funding acquisition.: **Gaël Le Roux:** Supervision, Methodology, Writing- Reviewing and Editing, Funding acquisition.

Data availability

Data is provided in the supplementary material and will be made available in the PANGEAE online database.

Declaration of competing interest

We declare that there are no conflicts of interest.

Acknowledgements

We would like to thank Marie-Jo Tavella (LEFE) for her assistance in the clean room laboratory, the Service ICP-MS of Observatoire Midi-Pyrénées Toulouse for ICP-MS analyses and Natalia Piotrowska (Gliwice University, POL) for pre-processing the GdA ^{14}C-samples. Our thanks also go to Chuxian Li for her help in the field, Mathias Bahns for solving technical issues, our friendly local contacts Ernst Partl and his staff at the Naturpark Kaunergrat and the Bezirkshauptmannschaft Landeck for permissions. We also thank Klaus Oeggl for providing us with detailed pollen information from the Piller Moor study by Hubmann (1994).

Funding

The main funding body was the German Research Foundation (DFG, project no. 39071778) within the GSC 208: "Graduate School for Integrated Studies of Human Development in Landscapes", funding the PhD-position of CvS. Funding for research visits of CvS between the partnering institutions was provided by Université Franco-Allemande (UFA/DFH; code CT-38-17) and by the German academic exchange service (DAAD) – "PPP: Frankreich" and by Campus France (PHC procope) 2017, for IU, FDV and CvS (project no. 57316724).

References

Artioli, G., Angelini, I., Nimis, P., Villa, I.M., 2016. A lead-isotope database of copper ores from the Southeastern Alps: A tool for the investigation of prehistoric copper metallurgy. J. Archaeol. Sci. 75, 27–39. https://doi.org/10.1016/j.jas.2016.09.005

Bao, K., Xing, W., Yu, X., Zhao, H., McLaughlin, N., Lu, X., Wang, G., 2012. Recent atmospheric dust deposition in an ombrotrophic peat bog in Great Hinggan Mountain, Northeast China. Sci. Total Environ. 431, 33–45. https://doi.org/https://doi.org/10.1016/j.scitotenv.2012.05.014

Bender, O., 2010. Entstehung, Entwicklung und Ende der alpinen Bergbauernkultur. Über das Entsteh. und die Endlichkeit Phys. Prozesse, Biol. Arten und Menschl. Kult. 113–137.

Blaauw, M., Christen, J.A., 2011. Flexible paleoclimate age-depth models using an autoregressive gamma process. Bayesian Anal. 6, 457–474. https://doi.org/10.1214/11-BA618

Bohdálková, L., Bohdálek, P., Břízová, E., Pacherová, P., Kuběna, A.A., 2018. Atmospheric metal pollution records in the Kovářská Bog (Czech Republic) as an indicator of anthropogenic activities over the last three millennia. Sci. Total Environ. 633, 857–874. https://doi.org/https://doi.org/10.1016/j.scitotenv.2018.03.142

527 Bortenschlager, S., 2010. Vegetationsgeschichte im Bereich des Rotmoostales, in: Koch, E.-M.,
528 Erschbaumer, B. (Eds.), Glaziale Und Periglaziale Lebensräume Im Raum Obergurgl. innsbruck
529 university press, Innsbruck, Austria, pp. 77–92.

530 Breitenlechner, E., Goldenberg, G., Lutz, J., Oeggl, K., 2013. The impact of prehistoric mining activities
531 on the environment: A multidisciplinary study at the fen Schwarzenbergmoos (Brixlegg, Tyrol,
532 Austria). Veg. Hist. Archaeobot. 22, 351–366. https://doi.org/10.1007/s00334-012-0379-6

533 Büntgen, U., Myglan, V.S., Ljungqvist, F.C., McCormick, M., Di Cosmo, N., Sigl, M., Jungclaus, J.,
534 Wagner, S., Krusic, P.J., Esper, J., Kaplan, J.O., De Vaan, M.A.C., Luterbacher, J., Wacker, L.,
535 Tegel, W., Kirdyanov, A. V., 2016. Cooling and societal change during the Late Antique Little Ice
536 Age from 536 to around 660 AD. Nat. Geosci. 9, 231–236. https://doi.org/10.1038/ngeo2652

537 Carvalho, F., Schulte, L., 2021. Reconstruction of mining activities in the Western Alps during the past
538 2500 years from natural archives. Sci. Total Environ. 750, 141208.
539 https://doi.org/https://doi.org/10.1016/j.scitotenv.2020.141208

540 Chambers, F.M., Booth, R.K., De Vleeschouwer, F., Lamentowicz, M., Le Roux, G., Mauquoy, D.,
541 Nichols, J.E., van Geel, B., 2012. Development and refinement of proxy-climate indicators from
542 peats. Quat. Int. 268, 21–33. https://doi.org/10.1016/j.quaint.2011.04.039

543 Damman, A.W.H., 1978. Distribution and Movement of Elements in Ombrotrophic Peat Bogs. Oikos
544 30, 480. https://doi.org/10.2307/3543344

545 De Vleeschouwer, F., Chambers, F.M., Swindles, G.T., 2010. Coring and sub-sampling of peatlands for
546 palaeoenvironmental research. Mires Peat 7, 1–10.

547 De Vleeschouwer, F., Gérard, L., Goormaghtigh, C., Mattielli, N., Le Roux, G., Fagel, N., 2007.
548 Atmospheric lead and heavy metal pollution records from a Belgian peat bog spanning the last
549 two millenia: human impact on a regional to global scale. Sci. Total Environ. 377, 282–295.
550 https://doi.org/10.1016/j.scitotenv.2007.02.017

551 Dietre, B., Walser, C., Kofler, W., Kothieringer, K., Hajdas, I., Lambers, K., Reitmaier, T., Haas, J.N.,
552 2017. Neolithic to Bronze Age (4850–3450 cal. BP) fire management of the Alpine Lower
553 Engadine landscape (Switzerland) to establish pastures and cereal fields. Holocene 27, 181–196.
554 https://doi.org/10.1177/0959683616658523

555 Dietre, B., Walser, C., Lambers, K., Reitmaier, T., Hajdas, I., Haas, J.N., 2014. Palaeoecological
556 evidence for Mesolithic to Medieval climatic change and anthropogenic impact on the Alpine
557 flora and vegetation of the Silvretta Massif (Switzerland/Austria). Quat. Int. 353, 3–16.
558 https://doi.org/10.1016/j.quaint.2014.05.001

559 Festi, D., Putzer, A., Oeggl, K., 2014. Mid and late holocene land-use changes in the Ötztal alps,
560 territory of the neolithic iceman "Ötzi." Quat. Int. 353, 17–33.
561 https://doi.org/10.1016/j.quaint.2013.07.052

562 Forel, B., Monna, F., Petit, C., Bruguier, O., Losno, R., Fluck, P., Begeot, C., Richard, H., Bichet, V.,
563 Chateau, C., 2010. Historical mining and smelting in the Vosges Mountains (France) recorded in
564 two ombrotrophic peat bogs. J. Geochemical Explor. 107, 9–20.
565 https://doi.org/10.1016/j.gexplo.2010.05.004

566 Fromme, G., 1957. Der Waldrückgang im Oberinntal (Tirol) Untersuchungen über das Ausmaß, die
567 Ursachen und Folgeerscheinungen des Wald? rückganges in einem Gebirgslande sowie über die
568 Aussichten der Wiederaufforstung von. Mitteilungen der Forstl. Bundesversuchsanstalt
569 Mariabrunn 54, 3–222.

570 Gałka, M., Aunina, L., Feurdean, A., Hutchinson, S., Kołaczek, P., Apolinarska, K., 2017. Rich fen
571 development in CE Europe, resilience to climate change and human impact over the last ca.
572 3500 years. Palaeogeogr. Palaeoclimatol. Palaeoecol. 473, 57–72.
573 https://doi.org/10.1016/j.palaeo.2017.02.030

574 Givelet, N., Le Roux, G., Cheburkin, A., Chen, B., Frank, J., Goodsite, M.E., Kempter, H., Krachler, M.,
575 Noernberg, T., Rausch, N., Rheinberger, S., Roos-Barraclough, F., Sapkota, A., Scholz, C., Shotyk,
576 W., 2004. Suggested protocol for collecting, handling and preparing peat cores and peat
577 samples for physical, chemical, mineralogical and isotopic analyses. J. Environ. Monit. 6, 481–
578 492. https://doi.org/10.1039/B401601G

579 Grabherr, G., 2006. Die Via Claudia Augusta in Nordtirol, in: Walde, E., Grabherr, G. (Eds.), Via Claudia
580 Augusta Und Römerstraßenforschung Im Östlichen Alpenraum. Athesia-Tyrolia Druck GmbH,
581 Innsbruck, pp. 37–284.

582 Grutsch, C., Martinek, K.P., 2012. Die Nordtiroler Kupfererzvorkommen westlich von Schwaz als
583 Rohstoffpotential der Bronzezeit, in: Oeggl, K., Schaffer, V. (Eds.), Die Geschichte Des Bergbaus
584 in Tirol Und Seinen Angrenzenden Gebieten, Proceedings Zum 6. Milestone-Meeting Des SFB
585 HiMAT Vom 3.-5.11.2011. innsbruck university press, Innsbruck, pp. 101–106.

586 Gstrein, P., 2013. About prehistoric Mining in Tyrol. Berichte der Geol. Bundesanstalt.

587 Guénette-Beck, B., Meisser, N., Curdy, P., 2009. New insights into the ancient silver production of the
588 Wallis area, Switzerland. Archaeol. Anthropol. Sci. 1, 215. https://doi.org/10.1007/s12520-009-
589 0014-3

590 Haditsch, J.G., Krainer, K., 1992. Jungalpidische Erzmineralisationen in der Phyllitgneiszone des

591 Arlberggebietes. Mitteilungen der Österreichischen Geol. Gesellschaft 84, 239–264.

592 Hammer, W., 1915. Über Gelbbleierz im Oberinntal. Zeitschrift des Ferdinandeums für Tirol und Vor.
593 3, 270–277.

594 Hanneberg, A., Simon, P., Wolkersdorfer, C., 2009. Galmei und schöne Wulfenite: Der Blei-Zink-
595 Bergbau rund um den Fernpass in Tirol. Lapis 34, 20.

596 Heiss, A.G., 2008. Weizen, Linsen, Opferbrote — Archäobotanische Analysen bronze- und
597 eisenzeitlicher Brandopferplätze im mittleren Alpenraum (PhD-Thesis). Universität Innsbruck.
598 https://doi.org/10.13140/RG.2.1.5185.5526

599 Helama, S., Jones, P.D., Briffa, K.R., 2017. Dark Ages Cold Period: A literature review and directions
600 for future research. Holocene 27, 1600–1606. https://doi.org/10.1177/0959683617693898

601 Hofmann, J., Wolkersdorfer, C., 2013. Der historische Bergbau im Montafon, Montafoner
602 Schriftenreihe. Heimatschutzverein Montafon, Schruns.

603 Hölzer, Adam, Hölzer, Amal, 1998. Silicon and titanium in peat profiles as indicators of human
604 impact. The Holocene 8, 685–696. https://doi.org/10.1191/095968398670694506

605 Höppner, B., Bartelheim, M., Huijsman, M., Krauss, R., Martinek, K.-P., Pernicka, E., Schwab, R., 2005.
606 Prehistoric copper production in the Inn Valley (Austria), and the earliest copper in Cental
607 Europe. Archaeometry 47, 293–315. https://doi.org/10.1111/j.1475-4754.2005.00203.x

608 Hubmann, G., 1994. Palynologische Untersuchunger zweier Sedimentprofile aus dem Oberen Inntal,
609 mit Augenmerk auf die anthropogene Beeinflussung (Diploma Thesis). University of Innsbruck.

610 Ivy-Ochs, S., Kerschner, H., Maisch, M., Christl, M., Kubik, P.W., Schlüchter, C., 2009. Latest
611 Pleistocene and Holocene glacier variations in the European Alps. Quat. Sci. Rev. 28, 2137–
612 2149. https://doi.org/10.1016/j.quascirev.2009.03.009

613 Jones, J.M., Hao, J., 1993. Ombrotrophic peat as a medium for historical monitoring of heavy metal
614 pollution. Environ. Geochem. Health 15, 67–74. https://doi.org/10.1007/BF02627824

615 Kalnicky, D.J., Singhvi, R., 2001. Field portable XRF analysis of environmental samples. J. Hazard.
616 Mater. 83, 93–122. https://doi.org/10.1016/S0304-3894(00)00330-7

617 Kapustová, V., Pánek, T., Hradecký, J., Zernitskaya, V., Hutchinson, S.M., Mulková, M., Sedláček, J.,
618 Bajer, V., 2018. Peat bog and alluvial deposits reveal land degradation during 16th-and 17th-
619 century colonisation of the Western Carpathians (Czech Republic). L. Degrad. Dev. 29, 894–906.
620 https://doi.org/10.1002/ldr.2909

621 Kempter, H., Görres, M., Frenzel, B., 1997. Ti and Pb concentrations in rainwater-fed bogs in Europe
622 as indicators of past anthropogenic activities. Water. Air. Soil Pollut. 100, 367–377.

623 Kempter, H., Krachler, M., Shotyk, W., 2010. Atmospheric Pb and Ti accumulation rates from
624 sphagnum moss: Dependence upon plant productivity. Environ. Sci. Technol. 44, 5509–5515.
625 https://doi.org/10.1021/es100366d

626 Kern, O.A., Koutsodendris, A., Süfke, F., Gutjahr, M., Mächtle, B., Pross, J., 2021. Persistent, multi-
627 sourced lead contamination in Central Europe since the Bronze Age recorded in the Füramoos
628 peat bog, Germany. Anthropocene 36, 100310.
629 https://doi.org/https://doi.org/10.1016/j.ancene.2021.100310

630 Knierzinger, W., Drescher-Schneider, R., Drollinger, S., Knorr, K.-H., Brunnbauer, L., Limbeck, A., Festi,
631 D., Horak, F., Wagreich, M., 2020. Anthropogenic and climate signals in late-Holocene peat
632 layers of an ombrotrophic bog in the Styrian Enns valley (Austrian Alps). E&G Quat. Sci. J. 69,
633 121–137. https://doi.org/10.5194/egqsj-69-121-2020

634 Knierzinger, W., Huang, J.-J.S., Strasser, M., Knorr, K.-H., Drescher-Schneider, R., Wagreich, M., 2021.
635 Late Holocene periods of copper mining in the Eisenerz Alps (Austria) deduced from calcareous
636 lake deposits. Anthropocene 33, 100273.

637 Koivula, M.P., Kujala, K., Rönkkömäki, H., Mäkelä, M., 2009. Sorption of Pb(II), Cr(III), Cu(II), As(III) to
638 peat, and utilization of the sorption properties in industrial waste landfill hydraulic barrier
639 layers. J. Hazard. Mater. 164, 345–352. https://doi.org/10.1016/j.jhazmat.2008.08.008

640 Krause, R., 1987. Early tin and copper metallurgy in south-western Germany at the beginning of the
641 Early Bronze Age, in: Old World Archaeometallurgy: Proceedings of the International
642 Symposium “Old World Archaeometallurgy,” Heidelberg. pp. 25–32.

643 Krumins, J., Robalds, A., 2015. Biosorption of Metallic Elements onto Fen Peat. Environ. Clim.
644 Technol. 14, 12–17. https://doi.org/doi:10.1515/rtuect-2014-0008

645 Kulikowski, M., 2012. 1 The Western Kingdoms, in: Johnson, S.F. (Ed.), The Oxford Handbook of Late
646 Antiquity. Oxford University Press, pp. 31–59.
647 https://doi.org/10.1093/oxfordhb/9780195336931.013.0001

648 Le Roux, G., Aubert, D., Stille, P., Krachler, M., Kober, B., Cheburkin, A., Bonani, G., Shotyk, W., 2005.
649 Recent atmospheric Pb deposition at a rural site in southern Germany assessed using a peat
650 core and snowpack, and comparison with other archives. Atmos. Environ. 39, 6790–6801.
651 https://doi.org/10.1016/j.atmosenv.2005.07.026

Le Roux, G., De Vleeschouwer, F., 2010. Preparation of peat samples for inorganic geochemistry used as palaeoenvironmental proxies. Mires Peat 7, 1–9.

Lichtenberger, E., 1965. Das Bergbauernproblem in den Österreichischen Alpen Perioden und Typen der Entsiedlung (The Problem of Mountain Farming in the Austrian Alps). Erdkunde 19, 39–57.

Liritzis, I., Zacharias, N., 2011. Portable XRF of archaeological artifacts: current research, potentials and limitations, in: Shackley, M. (Ed.), X-Ray Fluorescence Spectrometry (XRF) in Geoarchaeology. Springer, New York, pp. 109–142. https://doi.org/10.1007/978-1-4419-6886-9_6

Lomas-Clarke, S.H., Barber, K.E., 2007. Human impact signals from peat bogs–a combined palynological and geochemical approach. Veg. Hist. Archaeobot. 16, 419–429. https://doi.org/10.1007/s00334-006-0085-3

Longman, J., Ersek, V., Veres, D., 2020. High variability between regional histories of long-term atmospheric Pb pollution. Sci. Rep. 10, 1–10. https://doi.org/10.1038/s41598-020-77773-w

Lutz, J., Schwab, R., 2015. Eisenzeitliche Nutzung alpiner Kupferlagerstätten, in: Stöllner, T., Oeggl, K. (Eds.), Bergauf Bergab. 10.000 Jahre Bergbau in Den Ostalpen. Deutsches Bergbau-Museum Bochum, Bochum, pp. 113–116.

McLennan, S.M., 2001. Relationships between the trace element composition of sedimentary rocks and upper continental crust. Geochemistry, Geophys. Geosystems 2, 1021. https://doi.org/10.1029/2000GC000109

Mingram, J., Negendank, J.F.W., Brauer, A., Berger, D., Hendrich, A., Köhler, M., Usinger, H., 2007. Long cores from small lakes - Recovering up to 100 m-long lake sediment sequences with a high-precision rod-operated piston corer (Usinger-corer). J. Paleolimnol. 37, 517–528. https://doi.org/10.1007/s10933-006-9035-4

Monna, F., Petit, C., Guillaumet, J.-P., Jouffroy-Bapicot, I., Blanchot, C., Dominik, J., Losno, R., Richard, H., Lévêque, J., Chateau, C., 2004. History and Environmental Impact of Mining Activity in Celtic Aeduan Territory Recorded in a Peat Bog (Morvan, France). Environ. Sci. Technol. 38, 665–673. https://doi.org/10.1021/es034704v

More, A.F., Spaulding, N.E., Bohleber, P., Handley, M.J., Hoffmann, H., Korotkikh, E. V., Kurbatov, A. V., Loveluck, C.P., Sneed, S.B., McCormick, M., Mayewski, P.A., 2017. Next-generation ice core technology reveals true minimum natural levels of lead (Pb) in the atmosphere: Insights from the Black Death. GeoHealth 1, 211–219. https://doi.org/10.1002/2017GH000064

683 Nesbitt, H.W., Markovics, G., 1997. Weathering of granodioritic crust, long-term storage of elements
684 in weathering profiles, and petrogenesis of siliciclastic sediments. Geochim. Cosmochim. Acta
685 61, 1653–1670. https://doi.org/https://doi.org/10.1016/S0016-7037(97)00031-8

686 Neuhauser, G., 2015. ,,Argentifodinam seu montem dictum Mùntafùne ,, - 1000 Jahre Bergbau im
687 südlichen Vorarlberg, in: Stöllner, T., Oeggl, K. (Eds.), Bergauf Bergab. 10.000 Jahre Bergbau in
688 Den Ostalpen. Deutsches Bergbau-Museum Bochum, Bochum, pp. 447–454.

689 Nicolussi Castellan, S., Tomedi, G., Lachberger, R., 2008. Das bronzezeitliche Haus von Fließ-
690 Silberplan, in: Oeggl, K., Schaffer, V. (Eds.), Die Geschichte Des Bergbaus in Tirol Und Seinen
691 Angrenzenden Gebieten. Proceedings Zum 3. Milestone Meeting Des SFB HiMAT. p. 2008.

692 Nicolussi, K., Kaufmann, M., Patzelt, G., Van Der Plicht, J., Thurner, A., 2005. Holocene tree-line
693 variability in the Kauner Valley, Central Eastern Alps, indicated by dendrochronological analysis
694 of living trees and subfossil logs. Veg. Hist. Archaeobot. 14, 221–234.
695 https://doi.org/10.1007/s00334-005-0013-y

696 Nicolussi, K., Patzelt, G., 2000. Untersuchungen zur holozänen Gletscherentwicklung von Pasterze
697 und Gepatschferner (Ostalpen). Zeitschrift für Gletscherkd. und Glazialgeol. 36, 1–87.

698 Nieminen, T.M., Ukonmaanaho, L., Shotyk, W., 2002. Enrichment of Cu, Ni, Zn, Pb and As in an
699 ombrotrophic peat bog near a Cu-Ni smelter in Southwest Finland. Sci. Total Environ. 292, 81–
700 89. https://doi.org/10.1016/s0048-9697(02)00028-1

701 O'Brien, W., 2015. Prehistoric Copper Mining in Europe: 5500-500 BC. Oxford University Press.

702 Pacyna, J.M., Pacyna, E.G., 2001. An assessment of global and regional emissions of trace metals to
703 the atmosphere from anthropogenic sources worldwide. Environ. Rev. 9, 269–298.
704 https://doi.org/10.1139/er-9-4-269

705 Palmer, P.T., Jacobs, R., Baker, P.E., Ferguson, K., Webber, S., 2009. Use of field-portable XRF
706 analyzers for rapid screening of toxic elements in FDA-regulated products. J. Agric. Food Chem.
707 57, 2605–2613. https://doi.org/10.1021/jf803285h

708 Pernicka, E., Lutz, J., Stöllner, T., 2016. Bronze Age Copper Produced at Mitterberg, Austria, and its
709 Distribution. Archaeol. Austriaca 100, 19–55.

710 R Core Team, 2021. R: A Language and Environment for Statistical Computing.

711 Reimer, P.J., Austin, W.E.N., Bard, E., Bayliss, A., Blackwell, P.G., Bronk Ramsey, C., Butzin, M., Cheng,
712 H., Edwards, R.L., Friedrich, M., Grootes, P.M., Guilderson, T.P., Hajdas, I., Heaton, T.J., Hogg,
713 A.G., Hughen, K.A., Kromer, B., Manning, S.W., Muscheler, R., Palmer, J.G., Pearson, C., van der

714 Plicht, J., Reimer, R.W., Richards, D.A., Scott, E.M., Southon, J.R., Turney, C.S.M., Wacker, L.,
715 Adolphi, F., Büntgen, U., Capano, M., Fahrni, S.M., Fogtmann-Schulz, A., Friedrich, R., Köhler, P.,
716 Kudsk, S., Miyake, F., Olsen, J., Reinig, F., Sakamoto, M., Sookdeo, A., Talamo, S., 2020. THE
717 INTCAL20 NORTHERN HEMISPHERE RADIOCARBON AGE CALIBRATION CURVE (0–55 CAL kBP).
718 Radiocarbon 1–33. https://doi.org/DOI: 10.1017/RDC.2020.41

719 Reitmaier, T., 2012. Letzte Jäger, erste Hirten, in: Reitmaier, T. (Ed.), Letzte Jäger, Erste Hirten -
720 Hochalpine Archäologie in Der Silvretta. Archäologischer Dienst Graubünden, Chur, pp. 9–65.

721 Röpke, A., Stobbe, A., Oeggl, K., Kalis, A.J., Tinner, W., 2011. Late-holocene land-use history and
722 environmental changes at the high altitudes of st antönien (switzerland, northern alps):
723 Combined evidence from pollen, soil and tree-ring analyses. The Holocene 21, 485–498.
724 https://doi.org/10.1177/0959683610385727

725 Rothwell, J.J., Taylor, K.G., Chenery, S.R.N., Cundy, A.B., Evans, M.G., Allott, T.E.H., 2010. Storage and
726 behavior of As, Sb, Pb, and Cu in ombrotrophic peat bogs under contrasting water table
727 conditions. Environ. Sci. Technol. 44, 8497–8502.

728 Sapkota, A., Cheburkin, A.K., Bonani, G., Shotyk, W., 2007. Six millennia of atmospheric dust
729 deposition in southern South America (Isla Navarino, Chile). The Holocene 17, 561–572.
730 https://doi.org/https://doi.org/10.1177/0959683607078981

731 Schofield, J.E., Edwards, K.J., Mighall, T.M., Martínez Cortizas, A., Rodríguez-Racedo, J., Cook, G.,
732 2010. An integrated geochemical and palynological study of human impacts, soil erosion and
733 storminess from southern Greenland since c. AD 1000. Palaeogeogr. Palaeoclimatol. Palaeoecol.
734 295, 19–30. https://doi.org/10.1016/j.palaeo.2010.05.011

735 Segnana, M., Oeggl, K., Poto, L., Gabrieli, J., Festi, D., Kofler, W., Cesco Frare, P., Zaccone, C.,
736 Barbante, C., 2020. Holocene vegetation history and human impact in the eastern Italian Alps: a
737 multi-proxy study on the Coltrondo peat bog, Comelico Superiore, Italy. Veg. Hist. Archaeobot.
738 29, 407–426. https://doi.org/10.1007/s00334-019-00749-y

739 Shotyk, W., 1996. Natural and anthropogenic enrichments of As, Cu, Pb, Sb, and Zn in ombrotrophic
740 versus minerotrophic peat bog profiles, Jura Mountains, Switzerland. Water. Air. Soil Pollut. 90,
741 375–405. https://doi.org/10.1007/BF00282657

742 Shotyk, W., Blaser, P., Grünig, A., Cheburkin, A.K., 2000. A new approach for quantifying cumulative,
743 anthropogenic, atmospheric lead deposition using peat cores from bogs: Pb in eight Swiss peat
744 bog profiles. Sci. Total Environ. 249, 281–295. https://doi.org/10.1016/S0048-9697(99)00523-9

745 Shotyk, W., Krachler, M., Chen, B., 2004. Antimony in recent, ombrotrophic peat from Switzerland

and Scotland: Comparison with natural background values (5,320 to 8,020 14 C yr BP) and implications for the global atmospheric Sb cycle. Global Biogeochem. Cycles 18. https://doi.org/10.1029/2003GB002113

Shotyk, W., Krachler, M., Martinez-Cortizas, A., Cheburkin, A.K., Emons, H., 2002. A peat bog record of natural, pre-anthropogenic enrichments of trace elements in atmospheric aerosols since 12 370 14 C yr BP, and their variation with Holocene climate change. Earth Planet. Sci. Lett. 199, 21–37. https://doi.org/10.1016/S0012-821X(02)00553-8

Shotyk, W., Weiss, D., Appleby, P.G., Cheburkin, A.K., Frei, R., Gloor, M., Kramers, J.D., Reese, S., Van der Knaap, W.O., 1998. History of atmospheric lead depostion since 12,37014C yr BP from a Peat bog, Jura Mountains, Switzerland. Science (80-.). 281, 1635–1640. https://doi.org/10.1126/science.281.5383.1635

Sjögren, P., Knaap, W.O. Van Der, Leeuwen, J.F.N. Van, Andrič, M., Grünig, A., 2007. The occurrence of an upper decomposed peat layer, or “kultureller Trockenhorizont”, in the Alps and Jura Mountains. Mires Peat 2, 1–14.

Spitale, D., 2021. A warning call from mires of the Southern Alps (Italy): Impacts which are changing the bryophyte composition. J. Nat. Conserv. 61, 125994.

Staudt, M., 2011. Rätisches Haus in Wenns. Fundbericihte aus Österreich 49, 144–165.

Staudt, M., Tomedi, G., 2015. Zur Besiedlungsgeschichte der Ostalpen in der Mittel-bis Spätbronzezeit: Bestand, Kolonisation und wirtschaftlicher Neuanfang in der mittleren und späten Bronzezeit in Nordtirol, in: Stöllner, T., Oeggl, K. (Eds.), Bergauf Bergab. 10.000 Jahre Bergbau in Den Ostalpen. Deutsches Bergbau-Museum Bochum, Bochum, pp. 135–144.

Stöllner, T., 2015. die alpinen Kupfererzreviere: Aspekte ihrer zeitlichen, technologischen und wirtschaftlichen Entwicklung im zweiten Jahrtausend vor christus, in: Stöllner, T., Oeggl, K. (Eds.), Bergauf Bergab. 10.000 Jahre Bergbau in Den Ostalpen. Deutsches Bergbau-Museum Bochum, Bochum, pp. 99–104.

Stöllner, T., Oeggl, K., 2015. Bergauf Bergab. 10.000 Jahre Bergbau in den Ostalpen. Deutsches Bergbau-Museum Bochum, Bochum.

Sydow, W., 1995. Der hallstattzeitliche Bronzehort von Fliess im Oberinntal, Tirol. Fundberichte aus Österreich, Mater. A 3.

Thevenon, F., Guédron, S., Chiaradia, M., Loizeau, J.-L., Poté, J., 2011. (Pre-) historic changes in natural and anthropogenic heavy metals deposition inferred from two contrasting Swiss Alpine

777 lakes. Quat. Sci. Rev. 30, 224–233. https://doi.org/10.1016/j.quascirev.2010.10.013

778 Tomedi, G., 2012. Der mittelbronzezeitliche Schatzfund vom Piller., in: Hansen, S., Neumann, D.,
779 Vachta, T. (Eds.), Hort Und Raum: Aktuelle Forschungen Zu Bronzezeitlichen Deponierungen in
780 Mitteleuropa. Walter de Gruyter, Berlin, pp. 151–168.

781 Tomedi, G., 2002b. Hinweise zu einem lokalen Bronzehandwerk aus dem Depotfund vom
782 Moosbruckschrofen am Piller. Archaeo Tirol. Kleine Schriften 4 - Schriften zur Archäologischen
783 Landeskd. Tirols 4, 77–82.

784 Tomedi, G., Castellan, S.N., Lachberger, R., 2009. Denkmalschutzgrabungen am bronzezeitlichen Haus
785 von Fliess-Silberplan, Jahresbericht. Das Zentrum für Alte Kulturen. Innsbruck, Austria.

786 Tomedi, Gerhard, 2002a. Zur Datierung des Depotfundes vom Piller, in: Zeisler, J., Tomedi, G. (Eds.),
787 Archaeo Tirol. Kleine Schriften. Archäologische Forschungen Und Grabungsberichte Aus Tirol.
788 Wattens, pp. 43–46.

789 Tschurtschenthaler, M., Wein, U., 2002. Das Heiligtum auf der Pillerhöhe, in: Zemmer-Plank, L.,
790 Sölder, W. (Eds.), Kult Der Vorzeit in Den Alpen. Opfergaben - Opferplätze - Opferbrauchtum.
791 Volume 1. Athesia, Bozen, pp. 635–673.

792 Tschurtschenthaler, M., Wein, U., 1998. Das Heiligtum auf der Pillerhöhe und seine Beziehungen zur
793 Via Claudia Augusta, in: Walde, E. (Ed.), Via Claudia : Neue Forschungen. Innsbruck : Inst. für
794 Klassische Archäologie, Innsbruck, pp. 227–259.

795 Tschurtschenthaler, M., Wein, U., 1996. Kontinuität und Wandel eines alpinen Heiligtums im Laufe
796 seiner 1.800-jährigen Geschichte. Archäologie Österreichs 5, 14–28.

797 Ujević, I., Odžak, N., Barić, A., 2000. Trace metal accumulation in different grain size fractions of the
798 sediments from a semi-enclosed bay heavily contaminated by urban and industrial
799 wastewaters. Water Res. 34, 3055–3061. https://doi.org/https://doi.org/10.1016/S0043-
800 1354(99)00376-0

801 Valese, E., Conedera, M., Held, A.C., Ascoli, D., 2014. Fire, humans and landscape in the European
802 Alpine region during the Holocene. Anthropocene 6, 63–74.
803 https://doi.org/10.1016/j.ancene.2014.06.006

804 Vavtar, F., 1988. Die Erzanreicherungen im Nordtiroler Stubai-, Ötztal- und Silvrettakristallin, in:
805 Archiv Für Lagerstättenforschung. Archiv für Lagerstättenforschung. Geologisches Bundesamt,
806 Wien, pp. 103–153.

807 Viehweider, B., Feichter-Haid, A., Koch Waldner, T., Masur, A., 2013. Mining-related land use changes

since the Neolithic in the region of Kitzbühel (Tyrol). Metalla 20, 52–55.

von Klebelsberg, R., 1939. Nutzbare Bodenvorkommnisse in Nordtirol. Veröff. d. Museum Ferdinandeum Innsbruck, Bd 19, 1–56.

von Scheffer, C., Lange, A., De Vleeschouwer, F., Schrautzer, J., Unkel, I., 2019. 6200 years of human activities and environmental change in the northern central Alps. E&G Quat. Sci. J. 68, 13–28. https://doi.org/10.5194/egqsj-68-13-2019

von Srbik, R., 1929. Überblick des Bergbaues von Tirol und Vorarlberg in Vergangenheit und Gegenwart. Bericht des naturwissenschaftlich - medizinischen Vereins zu Innsbruck 41, 113–277.

Wahlmüller, N., 2002. Die Komperdellalm im Wandel der Jahrtausende. Ein Beitrag zur Vegetationsund Besiedlungsgeschichte des Oberen Gerichts, in: Klien, R. (Ed.), Serfaus. Athesia-Tyrolia Druck GmbH, Innsbruck: Gemeinde Serfaus, pp. 71–83.

Walde, C., 2006. Die Vegetations-und Siedlungsgeschichte im Oberen Gericht-Pollenanalytische Untersuchungen des Plemun-Weihers (Fließ, Tirol), in: Walde, E., Grabherr, G. (Eds.), Via Claudia Augusta Und Römerstraßenforschung Im Östlichen Alpenraum. Ikarus 1. Innsbruck University Press, pp. 394–407.

Wardenaar, E.C.P., 1987. A new hand tool for cutting peat profiles. Can. J. Bot. 65, 1772–1773. https://doi.org/10.1139/b87-243

Weber, L., Cerny, I., Ebner, F., Fritz, I., Göd, R., Götzinger, M.A., Gräf, W., Paar, W.H., Prohaska, W., Sachsenhofer, R.F., 1997. Metallogenetische Karte von Österreich 1: 500.000. Arch. für Lagerstättenforsch.

Weiss, D., Shotyk, W., Appleby, P.G., Kramers, J.D.A.N.D., Cheburkin, A.K., 1999. Atmospheric Pb deposition since the industrial revolution recorded by five Swiss peat profiles: Enrichment factors, fluxes, isotopic composition, and sources. Environ. Sci. Technol. 33, 1340–1352. https://doi.org/10.1021/es980882q

Wierschowski, L., 1994. Die historische Demographie - ein Schlüssel zur Geschichte? Bevölkerungsrückgang und Krise des Römischen Reiches im 3. Jh. n. Chr. Klio 76, 355.

Wolkersdorfer, C., 1991. Geschichte des Bergbaus im westlichen Mieminger Gebirge/Tirol. Aufschluss 42, 359–379.

Yang, G., Peng, C., Chen, H., Dong, F., Wu, N., Yang, Y., Zhang, Y., Zhu, D., He, Y., Shi, S., 2017. Qinghai–Tibetan Plateau peatland sustainable utilization under anthropogenic disturbances and

climate change. Ecosyst. Heal. Sustain. 3. https://doi.org/10.1002/ehs2.1263

ZAMG, 2018. ZAMG [WWW Document]. Klimadaten von Österreich, 1971 - 2000. URL www.zamg.ac.at (accessed 9.4.18).

Zemmer-Plank, L., 1992. Ein Waffenopfer der Fritzens-Sanzeno-Kultur in Wenns im Pitztal. Veröffentlichungen des Tiroler Landesmuseum 72, 231–249.

Zoller, H., Erny-Rodmann, C., Punchakunnel, P., 1996. The history of vegetation and land use in the Lower Engadine (Switzerland). Pollen records of the last 13000 years. Natl. der Schweiz 86.

Zuna, M., Mihaljevič, M., Šebek, O., Ettler, V., Handley, M., Navrátil, T., Goliáš, V., 2011. Recent lead deposition trends in the Czech Republic as recorded by peat bogs and tree rings. Atmos. Environ. 45, 4950–4958. https://doi.org/https://doi.org/10.1016/j.atmosenv.2011.06.007

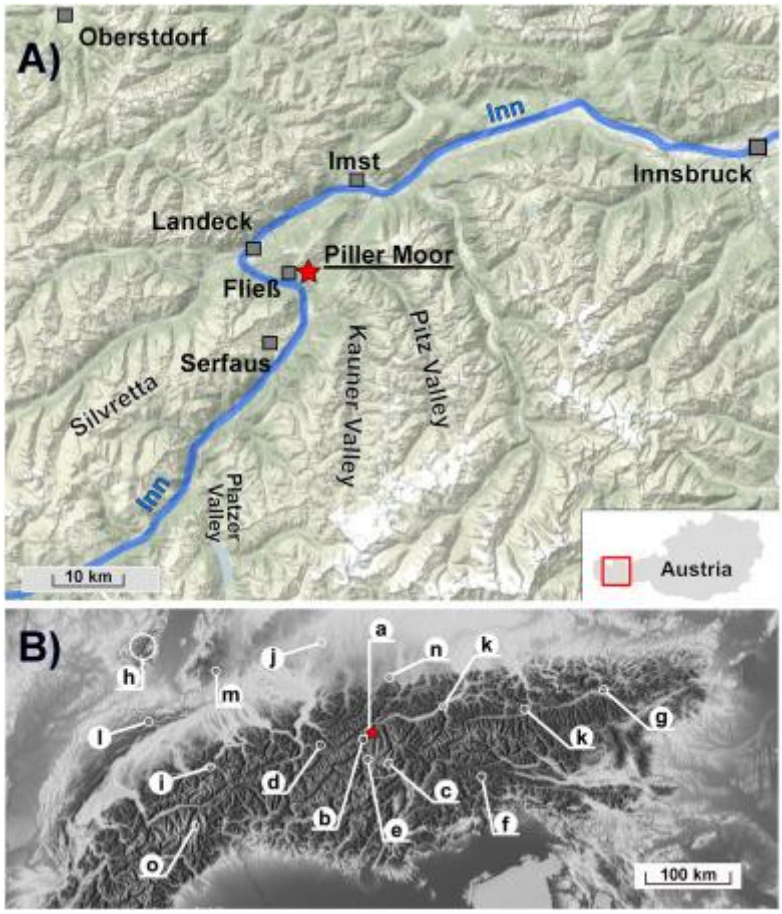

Figure 1: A) Northern Central Alps with study site (star). Edited from source: Stamen Design under CC-BY-3.0 and OSM contributors under ODbl. B) Selection of references in discussion. Palaeoenvironmental studies a) to d), metallurgy and Pb-accumulation e) to o). a: (Walde, 2006), b: (Wahlmüller, 2002) , c: (Festi et al., 2014), d: (Röpke et al., 2011), e: (Vavtar, 1988), f: (Segnana et al.,

2020), g: (Knierzinger et al., 2020), h: (Forel et al., 2010), i: (Carvalho and Schulte, 2021), j: (Kern et al., 2021), k: (Stöllner, 2015b), l: (Shotyk et al., 1998), m: (Le Roux et al., 2005), n: (Kempter et al., 2010), o: (More et al., 2017); background map openstreetmap.org, OSM contributors under ODbl.

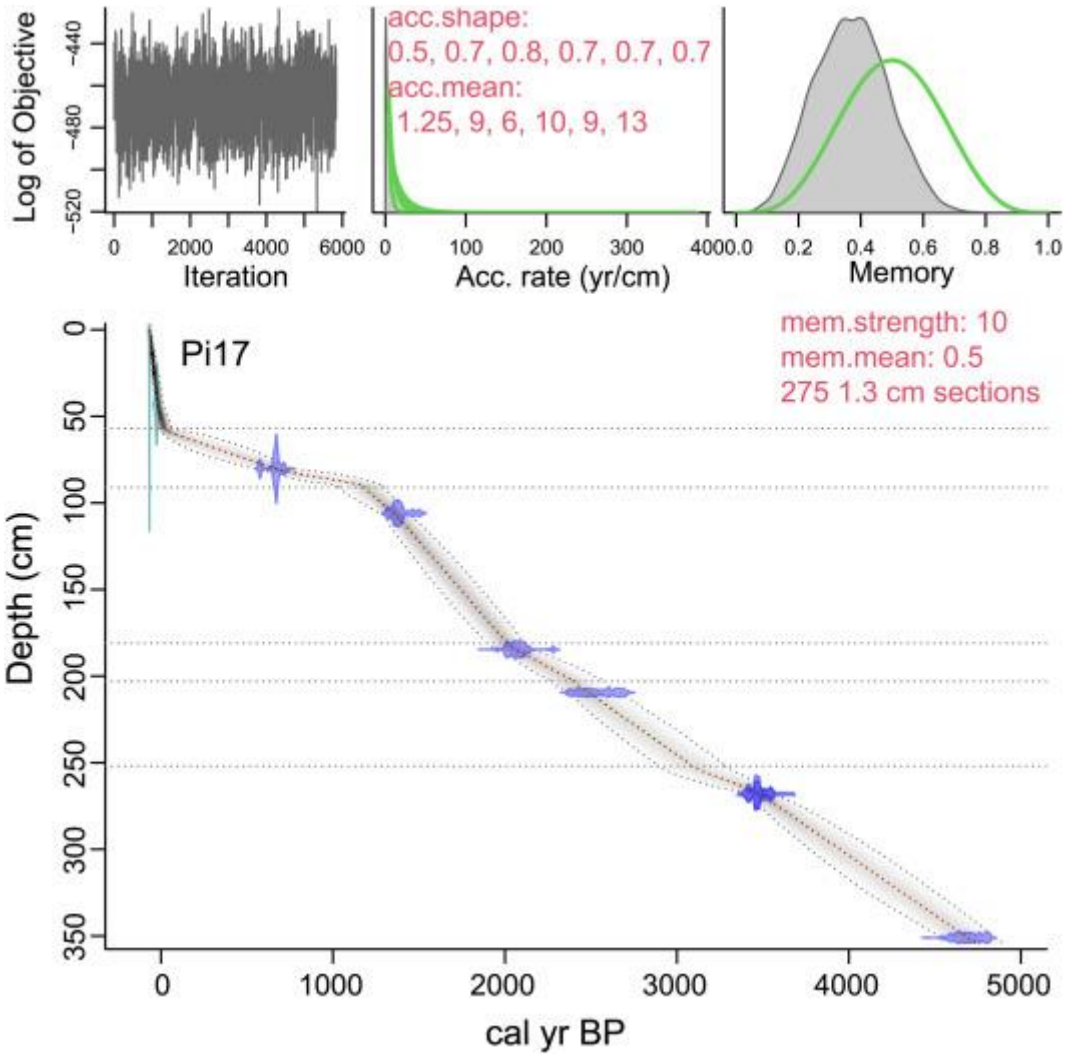

Figure 2: ADM of Pi17 composite core. Grey shaded area=95% within dotted line is the confidence interval. Dotted line in confidence interval is the median age. Dotted horizontal lines are boundaries between changes in core characteristics. Model input variables in red for the different sections between boundaries from top to bottom.

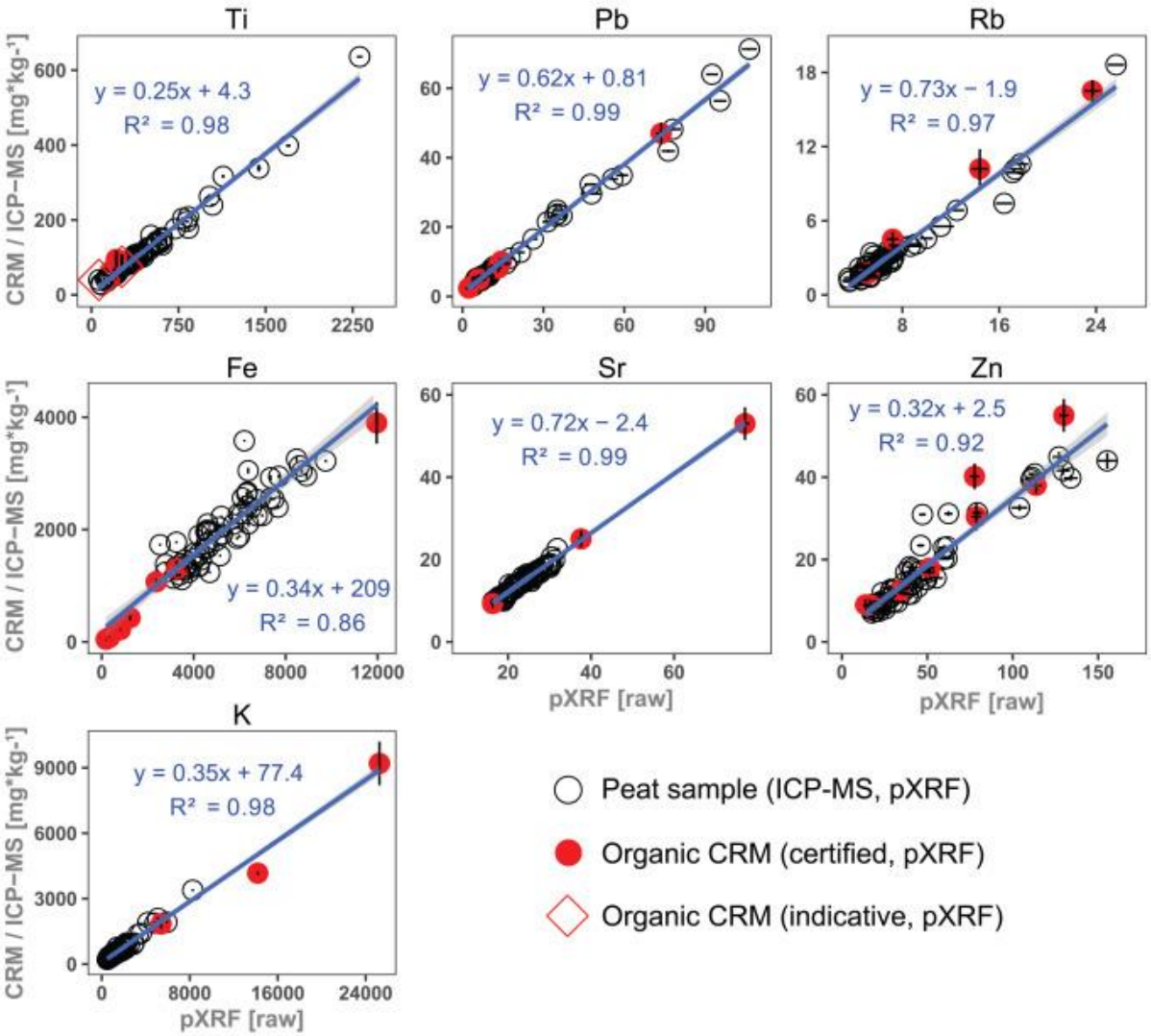

863

864 Figure 3: Cross-plots with regression analysis of ICP-MS and pXRF measurements. Open circles: peat,
865 filled red circles: CRMs in concentration range, blue lines: linear regressions. Error bars depict the
866 standard deviation of the measurements or the CRMs' errors.

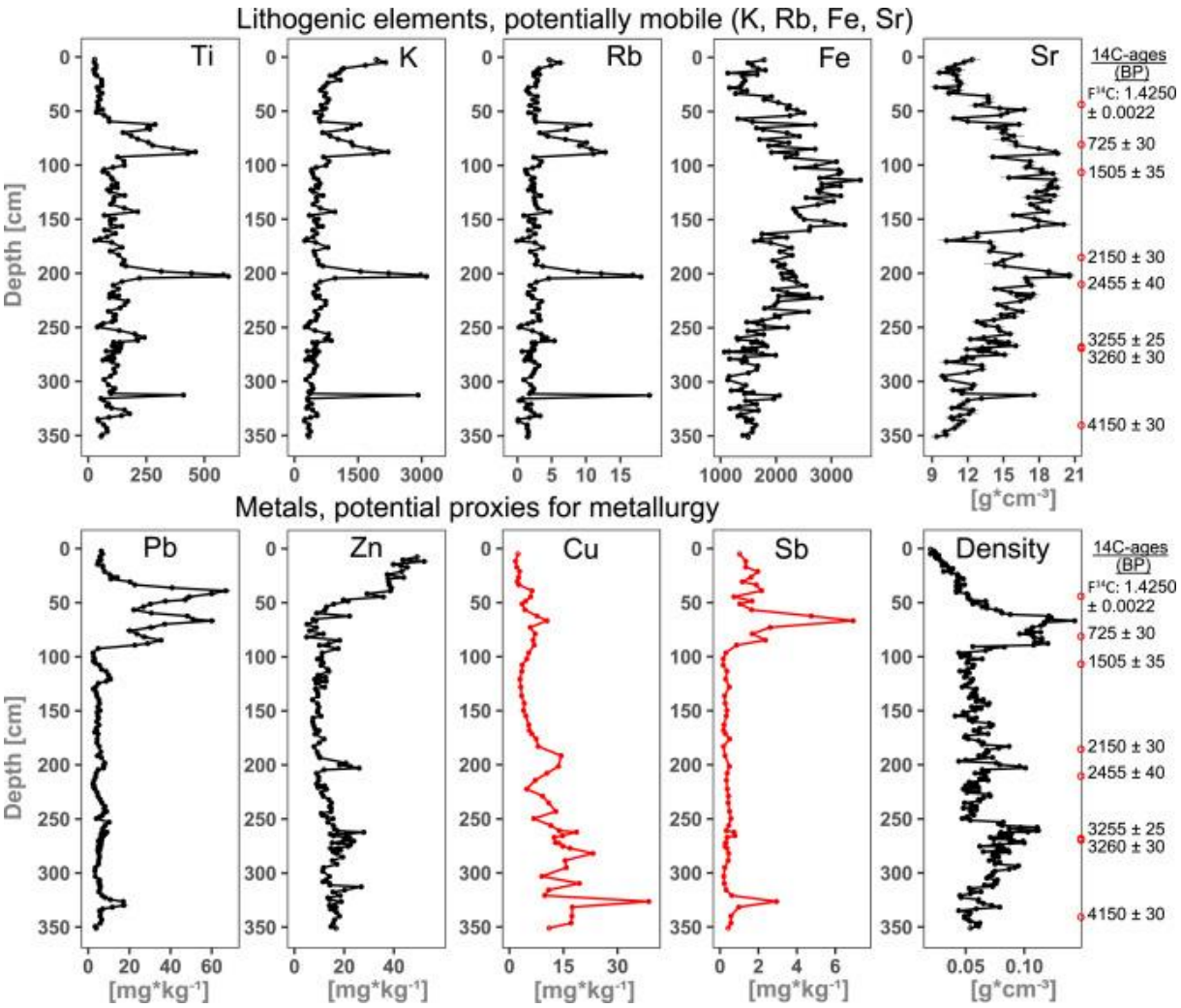

867

868 Figure 4: Piller Moor profiles of elements measured by pXRF (in black) and ICP-MS (in red) and dry bulk
869 density. $F^{14}C$ and ^{14}C-ages (cal BP) given on the right.

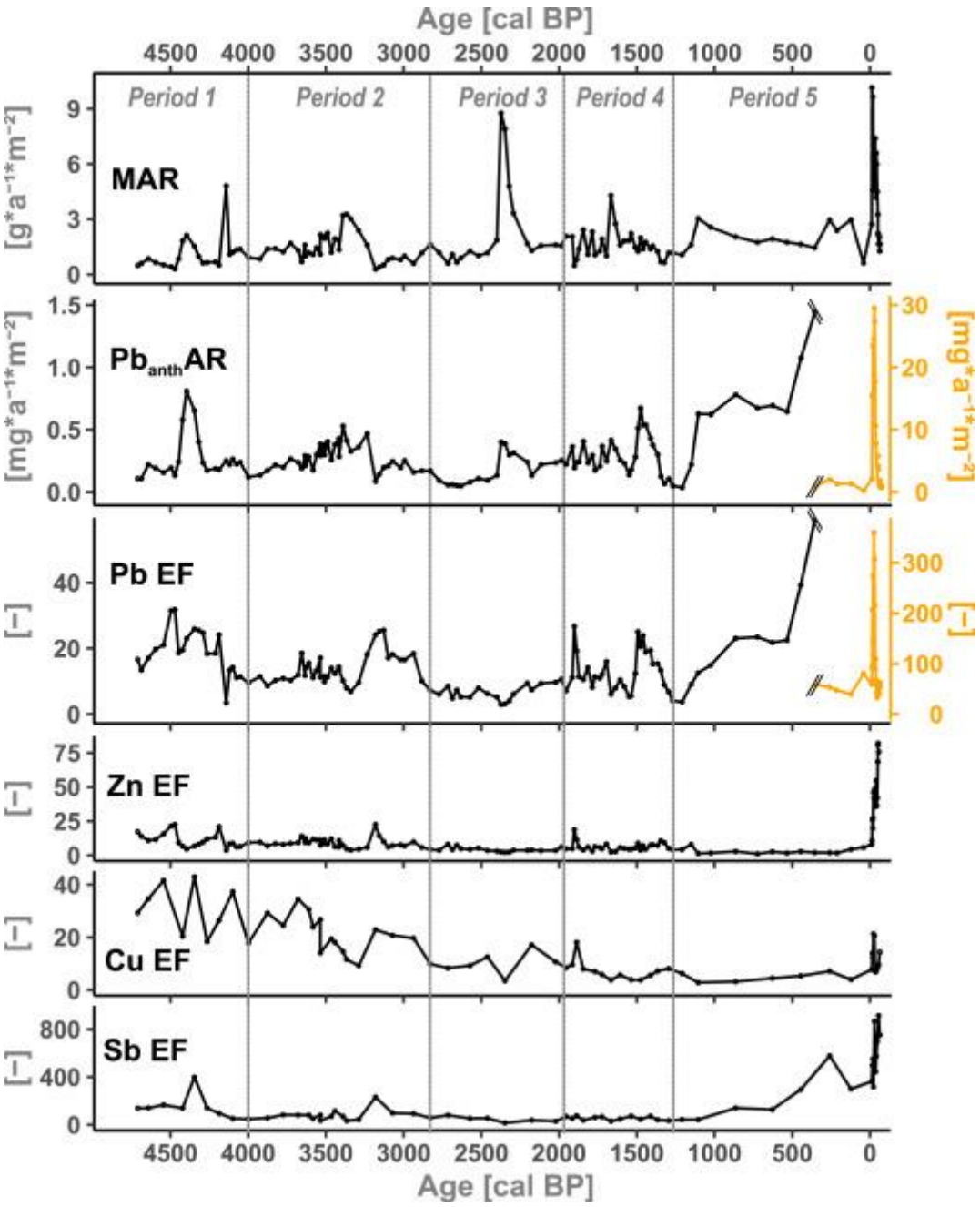

Figure 5: Mineral accumulation rate (MAR), anthropogenic Pb accumulation rate (Pb_{anth} AR) and metal enrichment factors (Pb EF, Zn EF, Cu EF, Sb EF). Orange lines (Pb AR and Pb E) zoomed in (secondary x-axis). Periods loosely correspond to cultural periods (e.g. Period 1 = Neolithic-Bronze Age transition; Period 2 = Bronze Age; Period 3 = Iron Age; Period 4 = Roman occupation in the Alps; Period 5 = Middle Ages to Postmodernity).

Table 1: Radiocarbon sample information on origin, depth, dated material and uncalibrated 14C-ages. Lab codes: GdA=Gliwice, Poz=Poznan. Depths of Poz-101726 and GdA-5493 are corrected to master

core A.

Lab. No.	Core	Depth [cm]	Material	^{14}C-age [BP]/F^{14}C	Comment
GdA-5492	Pi17A	43.2	*Sphagnum* spp. stems and leaves	1.4250 ± 0.0022	F14C Bomb pulse
Poz-99320	Pi17A	80.3	*Sphagnum* spp. stems and leaves	725 ± 30	0.5 mgC
GdA-5494	Pi17A	105.9	*Sphagnum* spp. stems and leaves	1505 ± 35	
Poz-101724	Pi17A	184.6	*Sphagnum* spp. stems and leaves	2150 ± 30	
GdA-5495	Pi17A	209.5	*Sphagnum* spp. stems and leaves	2455 ± 40	
GdA-5496	Pi17A	267.3	*Sphagnum* spp. stems and leaves	3255 ± 25	
Poz-101726	Pi17B	268.7	*Sphagnum* spp. stems and leaves, *Ericaceae* leaf	3260 ± 30	
GdA-5493	Pi17B	339.9	*Sphagnum* spp. stems and leaves	4150 ± 30	

Table 2: Synthesis of model estimates for approximates of average mineral and Pb_{anth}-accumulation rates and for the approximate cumulative deposition of Pb_{anth} within the periods 1 to 5 and in the most recent sample.

Period	Age [cal BP]	Estimated average MAR [g*m^{-2}*a^{-1}]	Estimated average Pb_{anth} AR [mg*m^{-2}*a^{-1}]	Estimated cumulative Pb_{anth} [g*m^{-2}]
1	4800–4000	1.01	0.26	0.19
2	4000–2800	1.94	0.33	0.4
3	2800–2000	1.84	0.16	0.12
4	2000–1300	1.41	0.25	0.17
5	After 1300	3.94	2.51	1.79
Surface	c. –65	1.6	1.21	**Total:** 2.68